HHS Public Access

Author manuscript

ACS Chem Biol. Author manuscript; available in PMC 2017 September 16.

Published in final edited form as:

ACS Chem Biol. 2016 September 16; 11(9): 2428–2437. doi:10.1021/acschembio.6b00539.

Semisynthetic and *in vitro* phosphorylation of alpha-synuclein at Y39 promotes functional partly-helical membrane-bound states resembling those induced by PD mutations

Igor Dikiy[a,‡,†], **Bruno Fauvet**[b,&,†], **Ana Jovičić**[c], **Anne-Laure Mahul-Mellier**[b], **Carole Desobry**[b], **Farah El-Turk**[b,§], **Aaron D. Gitler**[c], **Hilal A. Lashuel**[b,d,*], and **David Eliezer**[a,*]

[a]Department of Biochemistry and Program in Structural Biology, Weill Cornell Medical College, New York, NY 10065, United States [b]Laboratory of Molecular and Chemical Biology of Neurodegeneration, Ecole Polytechnique Fédérale de Lausanne, Station 19, CH-1015 Lausanne, Switzerland [c]Department of Genetics, Stanford University School of Medicine, Stanford, CA 94305, United States [d]Qatar Biomedical Research Institute (QBRI), Doha, Qatar

Abstract

Alpha-synuclein is a presynaptic protein of poorly understood function that is linked to both genetic and sporadic forms of Parkinson's disease. We have proposed that alpha-synuclein may function specifically at synaptic vesicles docked at the plasma membrane, and that the broken-helix state of the protein, comprising two antiparallel membrane-bound helices connected by a non-helical linker, may target the protein to such docked vesicles by spanning between the vesicle and the plasma membrane. Here we demonstrate that phosphorylation of alpha-synuclein at tyrosine 39, carried out by c-Abl *in vivo*, may facilitate interconversion of synuclein from the vesicle-bound extended-helix state to the broken-helix state. Specifically, in the presence of lipid vesicles Y39 phosphorylation leads to decreased binding of a region corresponding to helix-2 of the broken-helix state, potentially freeing this region of the protein to interact with other membrane surfaces. This effect is largely recapitulated by the phosphomimetic mutation Y39E and expression of this mutant in yeast results in decreased membrane localization. Intriguingly, the effects of Y39 phosphorylation on membrane binding closely resemble those of the recently reported disease linked mutation G51D. These findings suggest that Y39 phosphorylation could

[*]**Corresponding Authors**. dae2005@med.cornell.edu, hilal.lashuel@epfl.ch.

[‡]**Present Address**

Structural Biology Initiative, Advanced Science Research Center, City University of New York, New York, NY 10031, United States

[§]Department of Chemistry, University of Cambridge, Lensfield Road, CB2 1EW, Cambridge, United Kingdom

[&]Department of Plant Molecular Biology, University of Lausanne, Lausanne, Switzerland

[†]These authors contributed equally.

ASSOCIATED CONTENT

Supporting Information. Description of materials and methods and supplementary data is included. Supplementary Figures S1–S9: Membrane-bound states of aSyn. Semisynthesis of pY39 aSyn. Purity analysis of semisynthetic pY39 aSyn. Secondary structure of semisynthetic pY39 aSyn. Purity analysis of proteins prepared by *in vitro* phosphorylation. NMR comparison of WT, pY39 and Y39E aSyn in the free state. PRE of spin labeled aSyn bound to SDS micelles. Toxicity of aSyn Y39E in yeast. Characterization of the effect of Y39 phosphorylation on aSyn fibrillization propensity using semisynthetic pY39 aSyn. This material is available free of charge via the Internet at http://pubs.acs.org.

The authors declare no conflict of interest.

modulate functional aspects of alpha-synuclein, and perhaps influence pathological aggregation of the protein as well.

Alpha-synuclein (aSyn), a small (~15 kDa), soluble, presynaptic protein, is both genetically and pathologically linked to PD and other synucleinopathies, most notably by being found in proteinaceous aggregates in the surviving neurons of patients. While it is commonly accepted that a toxic gain of function associated with aggregate formation is the major contributor to synuclein toxicity, the native functions of aSyn remain poorly established. Understanding these functions may ultimately prove important in developing strategies to alter the behavior and/or aggregation of the protein *in vivo*.

Structurally, aSyn is an intrinsically-disordered protein and does not adopt any stable secondary or tertiary structure when isolated in dilute aqueous solution.[1,2] aSyn is N-terminally acetylated *in vivo* and exists mostly in the disordered, monomeric form,[3–5] although a dynamic interconversion between disordered monomers and helical tetramers has been proposed.[6,7] In addition, aSyn has been shown to bind synaptic vesicles/synaptosomes both *in vivo* and *in vitro*,[8–10] accompanied by a disorder-to-helix transition in the N-terminal ~100 residues.[1,11,12] In the presence of spheroidal lysophospholipid or detergent micelles, this N-terminal domain of aSyn adopts a broken-helix conformation consisting of two antiparallel helices (helix-1, res. 1–37; helix-2, res. 45–94) lying on the surface of the micelle.[11–14] When confronted with other, less highly-curved lipid topologies, such as those of bicelles or lipid vesicles, these antiparallel helices can fuse into an extended-helix conformation in which the linker becomes fully helical, connecting the entire N-terminal domain in one long helix (Fig. S1).[13,15–19]

Several studies over the years have implicated aSyn in vesicle trafficking and exocytosis or endocytosis,[20–23] and a recent study has posited a role for aSyn in promoting the formation of SNARE complexes.[24] We have shown that membrane-bound aSyn can interconvert between the broken- and extended-helix conformations depending on membrane topology and proposed that this process is important for its native function. In this model, the extended helix predominates on vesicle surfaces but converts into the broken-helix state when encountering two closely apposed membranes,[16,25,26] for example during docking, fusion or budding of synaptic vesicles at the plasma membrane. Thus, we posited that aSyn binds to synaptic vesicles in the extended-helix form and may help tether them to the presynaptic plasma membrane in the broken-helix form.

It follows that conversion between broken- and extended-helix states could be a point of regulation of synuclein function in response to cellular signaling events. Several kinases have been shown to phosphorylate aSyn on serine and tyrosine residues, mostly in the acidic C-terminal tail.[27–29] We recently showed that c-Abl phosphorylates aSyn at tyrosine 39, located in the linker region between helix-1 and helix-2,[30] a site that is well-positioned to influence the transition between extended and broken-helix states. Recent work has implicated c-Abl in neurodegenerative disorders such as Alzheimer's disease[31] and PD[32,33]. Increased c-Abl protein level and activation has been observed in the *substantia nigra* and striatum of PD patients, as well as in mice brains overexpressing aSyn,[33,34] and inhibition of c-Abl decreases the loss of dopaminergic neurons and promotes clearance of overexpressed

aSyn.[34] Moreover, we have recently shown that c-Abl phosphorylation of aSyn at Y39 regulates the clearance of aSyn protein by the autophagy and proteasome pathways.[30] Thus, phosphorylation of aSyn at Y39 by c-Abl may play important roles in both the normal function and pathological dysfunction of aSyn.

Here we investigate the effects of phosphorylation of aSyn at position 39, using semisynthetic pY39 aSyn, *in vitro* phosphorylated pY39 aSyn, and the phosphomimic mutant Y39E, on the structure of aSyn, with a focus on the lipid- and micelle-bound states. We find that phosphorylation at Y39 has a minimal effect on the ensemble of conformations aSyn adopts in aqueous solution, but a greater effect on the structure aSyn adopts in the presence of lipid membrane models. Specifically, Y39 phosphorylation disrupts binding of the linker region and the entire helix-2 to highly curved, negatively-charged lipid vesicles, possibly freeing helix-2 to interact with other membranes or potential protein binding partners. A reduction in membrane localization is also observed for the Y39E mutant expressed in yeast. These effects may have important repercussions for the function and dysfunction of aSyn.

RESULTS AND DISCUSSION

Protein semisynthesis achieves site-specific aSyn phosphorylation at Y39

Because c-Abl phosphorylates aSyn at Y125 as well as the primary site Y39,[30] we first opted for a three-fragment one-pot chemical protein semisynthesis strategy adapted from a previously described method,[35] to generate pY39 aSyn, with two ligation sites at A30 and A56 (Fig. S2A). This strategy relies on sequential NCL reactions: one between the recombinant fragment **1** comprising aSyn residues A56C-140 and fragment **2** comprising residues 31–55, containing the phosphotyrosine at position 39, resulting in fragment **4**; and one between this fragment **4** and fragment **3** (residues 1 to 29 with a C-terminal SR group, see SI). The fragments were designed to avoid problems associated with the synthesis of long peptides such as deletion sequences and other difficult to remove impurities. Using 4-mercaptophenylacetic acid (MPAA) as a NCL catalyst,[36] the first ligation between fragments **1** and **2**, occurring at a bulky valine residue at position 55, reached a satisfactory conversion rate after overnight incubation (Fig. S2B) to afford the intermediate ligation product Thz-aSyn(31–140) A56C pY39 (fragment **4**). Complete removal of the Thz protection was then performed by methoxylamine treatment, with the second ligation proceeding even faster and with good yield (Fig. S2C). The full-length ligation product was then desulfurized to regenerate the native alanine residues at positions 30 and 56 (Fig. S2D), and purification by RP-HPLC yielded 5.3 mg (0.36 μmol, 21.7%) of highly pure protein (Fig. S3).

pY39 has little or no effect on secondary structure in solution

Circular dichroism spectra of freshly-prepared WT and semisynthetic pY39 aSyn solutions were indistinguishable and typical of random coils (Fig. S4), indicating that phosphorylation at Y39 has no large impact on the global secondary structure content of aSyn. Like the WT protein, pY39 aSyn was also able to adopt highly helical structure upon binding to detergent micelles or highly negatively charged lipid vesicles.

Despite these similarities, we wished to investigate the structural effects of Y39 phosphorylation at higher resolution. NMR spectroscopy can provide residue-specific conformational details. However, because our synthesis strategy requires more than a third of the aSyn sequence to be prepared synthetically, the semisynthesis of isotopically-labeled, Y39-phosphorylated aSyn in quantities sufficient for NMR studies is prohibitively costly. Proteins for NMR were thus prepared by *in vitro* phosphorylation using SH2-CD c-Abl.[30,37] Obtaining site-specific phosphorylation at Y39 by *in vitro* phosphorylation required the Y125F/Y133F double mutation, to avoid previously observed phosphorylation at Y125[30] and, under preparative phosphorylation conditions (i.e. multiple additions of enzyme throughout the reaction process), at Y133. Y125 and Y133 are located in the C-terminal tail, which contributes little if at all to aSyn-membrane interactions, so these mutations are not expected to influence membrane binding. Indeed, mutation of all three Tyr residues in the C-terminal tail of aSyn to Phe has been shown to leave membrane-binding unperturbed[38]. Reactions were complete in about 6 hours and a single RP-HPLC purification step yielded pure pY39 aSyn Y125F/Y133F (Fig. S5A).

$^{1}H,^{15}N$-HSQC spectra of phosphorylated and unphosphorylated aSyn Y125F/Y133F in aqueous buffer (Fig. S6A) reveal only localized changes in the spectrum of the protein upon phosphorylation, restricted to the ~10 residues centered on Y39 (Fig. S6B). This extent of spectral changes is consistent with that seen for other phosphorylation sites in aSyn.[27,28] There is a very small increase in the helicity of some residues in the linker region upon phosphorylation (Fig. S6C) but no significant overall gain of secondary structure, consistent with our characterization of semisynthetic pY39 aSyn by CD.

Phosphorylation at Y39 perturbs the aSyn linker region in the presence of SDS micelles

In the presence of spheroidal SDS micelles, aSyn adopts a broken-helix conformation in which two helices connected by a non-helical linker, lie on the surface of a micelle in an antiparallel configuration.[12–14,39] CD spectroscopy revealed no detectable differences in helix formation upon SDS micelle binding between WT and semisynthetic pY39 aSyn (Fig. S4). A comparison of $^{1}H,^{15}N$-HSQC spectra of Y39 *in vitro* phosphorylated aSyn Y125F/Y133F and unphosphorylated WT aSyn in the presence of 40 mM SDS (Fig. 1A) reveals more extensive chemical shift perturbations than observed in the absence of SDS, suggesting a more widespread effect on the structure of the protein. These include small localized changes around the site of the Y125F and Y133F mutations (unrelated to phophorylation) and larger changes that localize to the phosphorylation site and extend approximately 10 residues to either side (Fig. 1B). This range includes the entire linker region as well as the C-terminal end of helix-1 and the N-terminal end of helix-2.

Alpha-carbon secondary shifts indicate that secondary structure of the two helices remains unchanged by phosphorylation, but helicity is increased in the linker region (Fig.1C) (average for res. 37–45 increases from 1.43 to 2.42 upon phosphorylation). Carbonyl carbon secondary shifts also indicate increased helicity in the linker (Fig. 1D) (average for res. 37–45 increases from 0.92 to 1.34 upon phosphorylation). These data suggest that phosphorylation of Y39 stabilizes helicity in the linker at concentrations of SDS expected to result in small, spheroidal micelles.

pY39 aSyn does not adopt extended-helix structure on spheroidal SDS micelles

When aSyn in the broken-helix state is labeled at the end of either helix-1 or helix-2 with a paramagnetic spin-label, a PRE effect can be seen on the other helix, since the two helices are within 25 Å of each other.[39] We prepared a Y39-phosphorylated aSyn 1–102 construct bearing a cysteine residue at position 9 (S9C), located in the helix-1 region of the broken-helix state, which was phosphorylated *in vitro*, purified by semipreparative HPLC (Fig. S5B), spin-labeled using MTSL, and assayed for intramolecular PRE effects in the presence of 40 mM SDS. Unphosphorylated protein exhibits a robust PRE effect for residues near the C-terminus of this construct, located near the end of helix-2 in the broken-helix state, and this effect was maintained to a similar extent upon phosphorylation at Y39 (Fig. 2A and Fig. S7A) indicating that micelle-bound pY39 aSyn still adopts the broken-helix state in which the N-terminus of helix-1 and the C-terminus of helix-2 are nearby in space. Introducing a spin label at position 83 near the end of helix-2 results in a PRE effect at the N-terminus of helix-1, which is again preserved upon phosphorylation (Fig. S7B). Another signature of the broken-helix state is a de-crease/interruption in sequential amide proton NOE peaks observed in the non-helical linker region.[11,12] Sequential NOEs from a ^{15}N-filtered HSQC-NOESY-HSQC experiment on pY39 aSyn were observed for the entire linker region, including relatively weak peaks for residues 41/42 and 42/43 (Fig. 2B). Similar data were obtained for WT aSyn in 40 mM SDS. Despite differences in absolute NOE intensity, likely due to slight differences in protein concentration, the pattern of sequential NOEs was the same for WT and pY39 aSyn (Fig. 2C). These results, combined with the PRE data, indicate that phosphorylation at Y39 does not change the conformation of the linker region previously observed for WT aSyn bound to detergent micelles.

The observation that pY39 phosphorylation does not disrupt the broken-helix structure of aSyn is important because this state is likely to be functionally important, and in particular may underlie aSyn's tight association with docked synaptic vesicles[40] and/or allow aSyn to mediate interactions between different membranes[16,25].

Phosphorylation at Y39 decreases helix-2 binding to lipid vesicles

Unphosphorylated aSyn has long been known to bind lipid vesicles containing negatively-charged headgroups, with a preference for more curved SUVs.[41–43] We examined whether such binding is affected by Y39 phosphorylation. We first used POPG vesicles with an average diameter of 100 nm to examine whether phosphorylation perturbs binding to very highly charged vesicles that are known to bind aSyn very strongly. The transition to α-helical structure upon addition of such vesicles, observed by CD spectroscopy, exhibited no difference between WT and semisynthetic pY39 aSyn (Fig. S4), likely because binding of the positively-charged aSyn N-terminus to such vesicles is very tight and not greatly affected by a change alteration of 1–2 charges.

Binding to SUVs prepared by sonication (diameter ~40 nm) composed of 15% DOPS/60% DOPC/25% DOPE, which more closely resemble synaptic vesicles, was monitored via intensity ratios of resonances in HSQC spectra obtained in the presence *versus* absence of vesicles. This assay provides a residue-by-residue readout of membrane-binding[44,45], unlike other methods that only report on binding of the protein as a whole. Unphosphorylated 15N-

labeled aSyn Y125F/Y133F in the presence of 3 mM SUVs (~30:1 lipid:protein) displays a binding profile (Fig. 3A) that is qualitatively similar to that of WT aSyn,[45–47] showing an unbound C-terminal ~40 residues and binding of the N-terminal domain that gradually and monotonically increases toward the N-terminus. In contrast, pY39 aSyn Y125F/Y133F shows a notably different binding profile (Fig. 3B). The very N-terminal residues bind to approximately the same extent as for the unphosphorylated protein, while a slight increase in the slope of the helix-1 region suggests a decrease in the binding cooperativity of this region, possibly as a result of fraying at the C-terminal end of helix-1. The most dramatic effect, however, is a clear disruption in binding starting at the phosphorylation site and continuing in the C-terminal direction through the remainder of helix-2, suggesting a significant population of phosphorylated protein in which helix-1 remains bound (though possibly frayed) while helix-2 dissociates from the membrane surface.

We estimated the bound populations of different binding modes by averaging the intensity ratios over different regions of the protein (see Materials and Methods in SI).[47] Using these populations, we then estimated an apparent binding constant for each binding mode (Table 1). The apparent K_D for all modes with binding at the N-terminus (“All bound states”) was very similar for unphosphorylated and phosphorylated proteins (6.4 vs 4.9 mM). However, phosphorylation resulted in a decrease in the apparent K_D for modes in which both helix-1 and helix-2 are bound (“Extended helix”) (18.4 vs 10.0 mM). These estimates were based on data obtained at a single lipid concentration because *in vitro* phosphorylated aSyn remains difficult to produce in large quantities needed for NMR titration experiments. We therefore generated a Y39E mutant as a potential mimic of the effects of phosphorylation at tyrosine 39. Glutamate is often used as a phosphomimic, although usually for serine or threonine phosphorylation.[28,29] We observed that the Y39E mutant behaved similarly to the *in vitro* phosphorylated protein inaqueous solution (Fig. S6) and when bound to SDS micelles (Figs. 1 and 2), as judged by NMR chemical shifts, PREs and NOEs, suggesting that mutant provides a reasonable mimic of the authentically phosphorylated protein.

We then made use of the Y39E mutant to obtain a more quantitative picture of how phosphorylation at Y39 may affect aSyn binding to lipid vesicles. The Y39E mutant bound in manner similar to that of pY39 aSyn, with the N-terminus binding to a similar extent as WT and a reduction in binding beyond the phosphorylation site extending through the helix-2 region (Fig. 3C,D). The populations of “All bound states” and “Extended helix” were calculated and fit to equation 3 (see Methods in SI) to extract apparent K_D values for the two states (Table 2), which, for WT, were close to our previously measured values[47]. The K_D value for the extended-helix state is also consistent with measurements obtained using CD titrations[48], which also monitor the formation of the extended-helix state, once the difference in membrane composition is taken into account[49]. The apparent K_D values for “All bound states” were very similar for WT and Y39E aSyn, whereas binding affinity for the “Extended helix” was decreased by more than a factor of 2 for the phosphomimic, as seen for the phosphorylated protein. Thus, the results obtained for the Y39E mutant using multiple lipid concentrations corroborate the effects observed using a single lipid concentration for the in vitro phosphorylated protein.

Although the effect of Y39E on membrane binding is qualitatively similar to the effect of Y39 phosphorylation (Fig. 3) we note that the reduction in the membrane affinity of the "Extended helix" state is larger for Y39E (Table 2) than for pY39 (Table 1). While the source of this difference is unclear at present, it could either result from the limitation of a having data at a single lipid concentration of analyzing the binding of pY39 aSyn, or it could reflect a real difference between the effects of the mutation and of authentic phosphorylation. The latter could be due to the shorter length of the Glu side chain, or to other differences between glutamate and phosphotyrosine.

Effects of Y39 on membrane binding resemble those of the G51D disease linked mutation

Binding of pY39 aSyn to SUVs that resemble the charged lipid composition of authentic synaptic vesicles is sharply reduced in a region beginning near the phosphorylation site and extending throughout the helix-2 region. This is reflected in an approximately two-fold increase in the apparent dissociation constant for the extended-helix bound state, while the apparent K_D value for binding of the very N-terminus of the protein (reflecting all bound states) remains similar to that measured previously for WT aSyn.[47] Phosphorylation of Y39 locally detaches the protein from the membrane surface and by doing so apparently terminates the propagation of helix formation and membrane binding from the region preceding the phosphorylation site, leaving the remainder of the lipid-binding domain (helix-2) free in solution.

Interestingly, we recently observed a very similar effect for the PD-associated synuclein mutation G51D.[50] Membrane binding is perturbed locally by this mutation, which prevents the extension of helical structure and membrane binding in the direction C-terminal to the mutation site. It appears likely that this effect is caused at least in part by local repulsion between the protein and the membrane due to the introduction of negative charge by phosphorylation or mutation. A similar effect was observed with the PD-linked helix-perturbing A30P mutant[46]. In general, there is now accruing evidence that helix formation upon membrane-binding by aSyn propagates from the N- to the C-terminus of the lipid binding domain, and that locally perturbing this process at any-point greatly decreases binding and helix formation of all residues C-terminal to the perturbation.

Phosphomimic Y39E mutation decreases aSyn membrane localization in yeast

Because the Y39E phosphomimic replicates the effect of pY39 on aSyn binding to lipid vesicles, we assessed the effect of this mutation in yeast, which have been used as a simple model system to monitor synuclein membrane binding in cells.[22,51,52] When expressed in yeast, aSyn exhibits a halo-like localization to the cell periphery.[52] PD-linked mutants with decreased membrane-binding capacity, such as A30P and G51D, exhibit a reduction in the peripheral membrane localization.[50] Having shown that the phosphomimic mutation Y39E, like pY39, is deficient in membrane binding *in vitro*, we expressed YFP-tagged aSyn Y39E in yeast and compared its localization with WT as well as the A30P and G51D PD-linked mutants. As expected,[44,50,52] WT aSyn localized to the cell periphery while the A30P and G51D mutants were found in the cytoplasm; aSyn Y39E appeared to exhibit an intermediate localization phenotype, with both cytoplasmic and peripheral localization, and quantification

confirmed this observation (Fig. 4). These results are consistent with the *in vitro* observations of perturbed membrane binding by aSyn Y39E.

Because A30P, Y39E and G51D perturb binding of the helix-2 region, but not, or less so, of the helix-1 region, to membranes, this suggests that synuclein's localization in yeast depends on a membrane-binding mode involving helix-2, perhaps in a membrane-spanning broken-helix configuration. Although yeast are not directly representitive of neurons, yeast cells have been extensively used as a model that recapitulates some of the cellular behavior of aSyn.[22,52] It is also notable that aSyn from brain does not co-purify with isolated synaptic vesicles, consistent with its weak affinity for lipid vesicles in vitro, but is instead found in synaptosomal fractions that contain vesicles stillattached to their associated membranes.[40] This suggests that in neurons, as well as in yeast, aSyn localization may depend on a binding mode involving more than just the vesicle membrane and that modifications that disrupt helix-2 binding to membranes (A30P, pY39, G51D) may perturb this localization in neurons.

Y39 phosphorylation may regulate aSyn function by releasing helix-2 from the membrane surface

Because Y39 is phosphorylated *in vivo* by c-Abl kinase, it appears likely that this phosphorylation event may regulate the physiological function(s) of aSyn. Reducing the affinity of helix-2 for membrane surfaces could play a functional role at the synapse by "freeing" this region of the protein, allowing it to engage in interactions with other membrane surfaces or protein binding partners. Based on the fact that helix-2 remains associated with the SDS micelle surface even upon phosphorylation, it appears that this segment of the protein is able, at least in some contexts, to bind membranes and form helical structure even when not coupled to the N-terminal helix-1 region. Such a binding event, perhaps assisted or mediated by protein-protein interactions involving the C-terminal tail, could lead to aSyn molecules spanning between different membranous organelles of distinct lipid composition and/or curvature, as we have proposed before.[25,26] Thus, phosphorylation by c-Abl at Y39 could represent a molecular switch that allows aSyn to alternate between its two membrane-bound states to regulate vesicle docking and/or aSyn protein-protein interactions.

Another potential consequence of Y39 phosphorylation is recognition by SH2 or other phosphotyrosine-binding motifs. For example, prediction of which SH2 domains may recognize the pY39 aSyn sequence using MoDPepInt[53] results in hits to the Lyn and Yes non-receptor tyrosine kinase SH2 domains. Both kinases are expressed in brain tissue[54] and may play an as yet unknown role in regulating aSyn biology, especially since other Src-family kinases are known to phosphorylate aSyn at Y125.

Y39 phosphorylation may alter aSyn toxicity

Y39 phosphorylation by c-Abl could also be involved in mediating aSyn-related toxicity in PD. The levels and activity of c-Abl have been shown to be correlated with the progression of PD,[33,34] while we and others have demonstrated that inhibition of phosphorylation of aSyn at Y39 by c-Abl leads to increased degradation of aSyn.[30,34] Interestingly, N-terminal partly-helical states have been linked to pathological aggregation of aSyn on membrane

surfaces[25,46] and at least two PD-linked mutations lead to the dramatic increase in the formation of such states.[46,50] However, a recent study shows that formation of partly-helical states is not in-and-of itself sufficient for promoting membrane-induced aggregation.[55] Thus the relationship between the partly-helical states promoted by Y39 phosphorylation and aSyn aggregation will have to be examined carefully in different contexts to determine whether this effect may contribute to decreased clearance of aSyn upon inhibition of c-Abl activity.

Interestingly, we observed that the phosphomimic aSyn mutant Y39E shows decreased toxicity in yeast compared to WT protein (Fig. S8), as measured by yeast spotting assays, with an effect similar to that observed for the G51D mutant. This effect could be explained in part by a decreased aggregation propensity of the membrane-free protein, as we noted that pY39 aSyn aggregates much more slowly than the WT protein in solution (Fig. S9). It could also be related to phosphorylation-induced changes in turnover rates, as recently reported for S129 phosphorylation.[56] However, a more systematic study of aSyn mutants in yeast showed no correlation between fibrillization lag time and yeast toxicity; instead, the correlation was between membrane binding and toxicity.[57] Our findings with aSyn Y39E support this observation. To what extent this correlation is transferable to neurons, and the potential involvement of partly-helical states in yeast or neuron toxicity, remains to be established.

Conclusions

Phosphorylation of aSyn at Y39 has effects that could modulate both the function and dysfunction of aSyn. On the functional side, Y39 phosphorylation could regulate differential binding of the helix-2 region of the N-terminal domain to lipid membranes, potentially influencing the interaction of aSyn with docked synaptic vesicles and the plasma membrane. This in turn could regulate the potential, but still poorly understood, activities of aSyn in either promoting or inhibiting vesicle release[25,58]. On the pathological side, pY39 aSyn is far less prone to aggregate in the free state, but promotes partly-helical membrane-bound states that may influence aggregation *in vivo*. The Y39E mutation mimics many of the effects of Y39 phosphorylation *in vitro* and exhibits decreased toxicity compared to WT aSyn in yeast, but the relationships between membrane-binding, aggregation, toxicity in yeast, and toxicity in humans remain to be determined.

Finally, it appears clear that c-Abl is involved the etiology of PD, but it is unclear whether increased c-Abl activity is a cause or effect of the disease state. If the major effect of c-Abl mediated phosphorylation of aSyn at Y39 is on function, increased c-Abl activity in PD could be a sign of the system attempting to counteract a loss of aSyn function during the course of the disease. If the major effect is on the formation of one or more pathological states, increased c-Abl phosphorylation of aSyn in PD may be directly causative. These questions underline the importance of a more complete understanding of the interplay between c-Abl and aSyn function and pathology.

Supplementary Material

Refer to Web version on PubMed Central for supplementary material.

Acknowledgments

Funding Sources

This work was supported by NIH/NIA grants R37AG019391 and R01AG025440 (DE), the Irma T. Hirschl Foundation (DE), the Swiss National Science Foundation grants 315230-125483 (HAL), the European Research Council, ERC starting grant 243182 (BF, HAL, AMM), and the Michael J. Fox Foundation (HAL). D.E. is a member of the New York Structural Biology Center. The data collected at NYSBC was made possible by a grant from NYSTAR and ORIP/NIH facility improvement grant CO6RR015495. The 900 MHz NMR spectrometers were purchased with funds from NIH grant P41GM066354, the Keck Foundation, New York State Assembly, and U.S. Dept. of Defense.

We gratefully acknowledge T. F. Ramlall for significant help with protein production, D. Snead for stimulating discussions, and Drs. C. Bracken and S. Bhattacharya for help with NMR experiments.

REFERENCES

1. Eliezer D, Kutluay E, Bussell R, Browne G. Conformational properties of α-synuclein in its free and lipid-associated states. J. Mol. Biol. 2001; 307:1061–1073. [PubMed: 11286556]
2. Weinreb PH, Zhen W, Poon AW, Conway KA, Lansbury PT Jr. NACP, a protein implicated in Alzheimer's disease and learning, is natively unfolded. Biochemistry. 1996; 35:13709–13715. [PubMed: 8901511]
3. Binolfi A, Theillet F-X, Selenko P. Bacterial in-cell NMR of human α-synuclein: a disordered monomer by nature? Biochem. Soc. Trans. 2012; 40:950–954. [PubMed: 22988846]
4. Fauvet B, Fares M-B, Samuel F, Dikiy I, Tandon A, Eliezer D, Lashuel HA. Characterization of semisynthetic and naturally Nα-acetylated α-synuclein in vitro and in intact cells: implications for aggregation and cellular properties of α-synuclein. J. Biol. Chem. 2012; 287:28243–28262. [PubMed: 22718772]
5. Fauvet B, Mbefo M, Fares M-B, Desobry C, Michael S, Ardah M, Tsika E, Coune P, Prudent M, Lion N, Eliezer D, Moore D, Schneider B, Aebischer P, El-Agnaf O, Masliah E, Lashuel H. α-Synuclein in Central Nervous System and from Erythrocytes, Mammalian Cells, and Escherichia coli Exists Predominantly as Disordered Monomer. J. Biol. Chem. 2012; 287:15345–15364. [PubMed: 22315227]
6. Bartels T, Choi J, Selkoe D. alpha-Synuclein occurs physiologically as a helically folded tetramer that resists aggregation. Nature. 2011; 477:107–110. [PubMed: 21841800]
7. Wang W, Perovic I, Chittuluru J, Kaganovich A, Nguyen L, Liao J, Auclair J, Johnson D, Landeru A, Simorellis A, Ju S, Cookson M, Asturias F, Agar J, Webb B, Kang C, Ringe D, Petsko G, Pochapsky T, Hoang Q. A soluble α-synuclein construct forms a dynamic tetramer. Proc. Natl. Acad. Sci. U.S.A. 2011; 108:17797–17802. [PubMed: 22006323]
8. Irizarry MC, Kim TW, McNamara M, Tanzi RE, George JM, Clayton DF, Hyman BT. Characterization of the precursor protein of the non-A beta component of senile plaques (NACP) in the human central nervous system. J. Neuropathol. Exp. Neurol. 1996; 55:889–895. [PubMed: 8759778]
9. Kahle PJ, Neumann M, Ozmen L, Müller V, Jacobsen H, Schindzielorz A, Okochi M, Leimer U, Putten Hvd, Probst A, Kremmer E, Kretzschmar HA, Haass C. Subcellular Localization of Wild-Type and Parkinson's Disease-Associated Mutant α-Synuclein in Human and Transgenic Mouse Brain. J. Neurosci. 2000; 20:6365–6373. [PubMed: 10964942]
10. Maroteaux L, Campanelli JT, Scheller RH. Synuclein: a neuron-specific protein localized to the nucleus and presynaptic nerve terminal. J. Neurosci. 1988; 8:2804–2815. [PubMed: 3411354]
11. Bussell R, Eliezer D. A Structural and Functional Role for 11-mer Repeats in α-Synuclein and Other Exchangeable Lipid Binding Proteins. J. Mol. Biol. 2003; 329:763–778. [PubMed: 12787676]
12. Chandra S, Chen X, Rizo J, Jahn R, Südhof TC. A broken alpha-helix in folded alpha-Synuclein. J. Biol. Chem. 2003; 278:15313–15318. [PubMed: 12586824]

13. Borbat P, Ramlall TF, Freed JH, Eliezer D. Inter-helix distances in lysophospholipid micelle-bound alpha-synuclein from pulsed ESR measurements. J. Am. Chem. Soc. 2006; 128:10004–10005. [PubMed: 16881616]

14. Ulmer T, Bax A, Cole N, Nussbaum R. Structure and Dynamics of Micelle-bound Human α-Synuclein. J. Biol. Chem. 2005; 280:9595–9603. [PubMed: 15615727]

15. Georgieva E, Ramlall T, Borbat P, Freed J, Eliezer D. Membrane-Bound α-Synuclein Forms an Extended Helix: Long-Distance Pulsed ESR Measurements Using Vesicles, Bicelles, and Rodlike Micelles. J. Am. Chem. Soc. 2008; 130:12856–12857. [PubMed: 18774805]

16. Georgieva E, Ramlall T, Borbat P, Freed J, Eliezer D. The lipid-binding domain of wild type and mutant alpha-synuclein: compactness and interconversion between the broken and extended helix forms. J. Biol. Chem. 2010; 285:28261–28274. [PubMed: 20592036]

17. Jao CC, Hegde BG, Chen J, Haworth IS, Langen R. Structure of membrane-bound alpha-synuclein from site-directed spin labeling and computational refinement. Proc. Natl. Acad. Sci. U.S.A. 2008; 105:19666–19671. [PubMed: 19066219]

18. Ferreon AC, Gambin Y, Lemke EA, Deniz AA. Interplay of alpha-synuclein binding and conformational switching probed by single-molecule fluorescence. Proc Natl Acad Sci U S A. 2009; 106:5645–5650. [PubMed: 19293380]

19. Trexler AJ, Rhoades E. Alpha-synuclein binds large unilamellar vesicles as an extended helix. Biochemistry. 2009; 48:2304–2306. [PubMed: 19220042]

20. Busch DJ, Oliphint PA, Walsh RB, Banks SML, Woods WS, George JM, Morgan JR. Acute increase of α-synuclein inhibits synaptic vesicle recycling evoked during intense stimulation. Mol. Biol. Cell. 2014; 25:3926–3941. [PubMed: 25273557]

21. Cabin DE, Shimazu K, Murphy D, Cole NB, Gottschalk W, McIlwain KL, Orrison B, Chen A, Ellis CE, Paylor R, Lu B, Nussbaum RL. Synaptic Vesicle Depletion Correlates with Attenuated Synaptic Responses to Prolonged Repetitive Stimulation in Mice Lacking α-Synuclein. J. Neurosci. 2002; 22:8797–8807. [PubMed: 12388586]

22. Cooper AA, Gitler AD, Cashikar A, Haynes CM, Hill KJ, Bhullar B, Liu K, Xu K, Strathearn KE, Liu F, Cao S, Caldwell KA, Caldwell GA, Marsischky G, Kolodner RD, Labaer J, Rochet J-C, Bonini NM, Lindquist S. Alpha-synuclein blocks ER-Golgi traffic and Rab1 rescues neuron loss in Parkinson's models. Science. 2006; 313:324–328. [PubMed: 16794039]

23. Murphy DD, Rueter SM, Trojanowski JQ, Lee VM. Synucleins are developmentally expressed, and alpha-synuclein regulates the size of the presynaptic vesicular pool in primary hippocampal neurons. J. Neurosci. 2000; 20:3214–3220. [PubMed: 10777786]

24. Burré J, Sharma M, Tsetsenis T, Buchman V, Etherton M, Südhof T. α-Synuclein Promotes SNARE-Complex Assembly in Vivo and in Vitro. Science. 2010; 329:1663–1667. [PubMed: 20798282]

25. Dikiy I, Eliezer D. Folding and misfolding of alpha-synuclein on membranes. Biochim. Biophys. Acta. 2012; 1818:1013–1018. [PubMed: 21945884]

26. Eliezer, D. Protein folding and aggregation in in vitro models of Parkinson's Disease: Structure and function of alpha-synuclein. In: Nass, R.; Przedborski, S., editors. Parkinson's Disease: molecular and therapeutic insights from model systems. 1. Academic Press; 2008. p. 575-595.

27. Hejjaoui M, Butterfield S, Fauvet B, Vercruysse F, Cui J, Dikiy I, Prudent M, Olschewski D, Zhang Y, Eliezer D, Lashuel H. Elucidating the Role of C-Terminal Post-Translational Modifications Using Protein Semisynthesis Strategies: α-Synuclein Phosphorylation at Tyrosine 125. J. Am. Chem. Soc. 2012; 134:5196–5210. [PubMed: 22339654]

28. Paleologou K, Oueslati A, Shakked G, Rospigliosi C, Kim H-Y, Lamberto G, Fernandez C, Schmid A, Chegini F, Gai WP, Chiappe D, Moniatte M, Schneider B, Aebischer P, Eliezer D, Zweckstetter M, Masliah E, Lashuel H. Phosphorylation at S87 is enhanced in synucleinopathies, inhibits alpha-synuclein oligomerization, and influences synuclein-membrane interactions. J. Neurosci. 2010; 30:3184–3198. [PubMed: 20203178]

29. Paleologou K, Schmid A, Rospigliosi C, Kim H-Y, Lamberto G, Fredenburg R, Lansbury P, Fernandez C, Eliezer D, Zweckstetter M, Lashuel H. Phosphorylation at Ser-129 but Not the Phosphomimics S129E/D Inhibits the Fibrillation of α-Synuclein. J. Biol. Chem. 2008; 283:16895–16905. [PubMed: 18343814]

30. Mahul-Mellier A-L, Fauvet B, Gysbers A, Dikiy I, Oueslati A, Georgeon S, Lamontanara AJ, Bisquertt A, Eliezer D, Masliah E, Halliday G, Hantschel O, Lashuel HA. c-Abl phosphorylates α-synuclein and regulates its degradation: implication for α-synuclein clearance and contribution to the pathogenesis of Parkinson's disease. Hum. Mol. Genet. 2014; 23:2858–2879. [PubMed: 24412932]
31. Estrada LD, Zanlungo SM, Alvarez AR. C-Abl tyrosine kinase signaling: a new player in AD tau pathology. Curr. Alzheimer Res. 2011; 8:643–651. [PubMed: 21605041]
32. Imam SZ, Zhou Q, Yamamoto A, Valente AJ, Ali SF, Bains M, Roberts JL, Kahle PJ, Clark RA, Li S. Novel regulation of parkin function through c-Abl-mediated tyrosine phosphorylation: implications for Parkinson's disease. J. Neurosci. 2011; 31:157–163. [PubMed: 21209200]
33. Ko HS, Lee Y, Shin J-H, Karuppagounder SS, Gadad BS, Koleske AJ, Pletnikova O, Troncoso JC, Dawson VL, Dawson TM. Phosphorylation by the c-Abl protein tyrosine kinase inhibits parkin's ubiquitination and protective function. Proc. Natl. Acad. Sci. U.S.A. 2010; 107:16691–16696. [PubMed: 20823226]
34. Hebron ML, Lonskaya I, Moussa CEH. Nilotinib reverses loss of dopamine neurons and improves motor behavior via autophagic degradation of α-synuclein in Parkinson's disease models. Hum. Mol. Genet. 2013; 22:3315–3328. [PubMed: 23666528]
35. Fauvet B, Butterfield SM, Fuks J, Brik A, Lashuel HA. One-pot total chemical synthesis of human α-synuclein. Chem. Commun. 2013; 49:9254–9256.
36. Johnson ECB, Kent SBH. Insights into the mechanism and catalysis of the native chemical ligation reaction. J. Am. Chem. Soc. 2006; 128:6640–6646. [PubMed: 16704265]
37. Seeliger MA, Young M, Henderson MN, Pellicena P, King DS, Falick AM, Kuriyan J. High yield bacterial expression of active c-Abl and c-Src tyrosine kinases. Protein Sci. 2005; 14:3135–3139. [PubMed: 16260764]
38. Sevcsik E, Trexler AJ, Dunn JM, Rhoades E. Allostery in a disordered protein: oxidative modifications to alpha-synuclein act distally to regulate membrane binding. J Am Chem Soc. 2011; 133:7152–7158. [PubMed: 21491910]
39. Bussell R, Ramlall TF, Eliezer D. Helix periodicity, topology, and dynamics of membrane-associated alpha-synuclein. Protein Sci. 2005; 14:862–872. [PubMed: 15741347]
40. Burré J, Sharma M, Südhof TC. α-Synuclein assembles into higher-order multimers upon membrane binding to promote SNARE complex formation. Proc. Natl. Acad. Sci. U.S.A. 2014; 111:E4274–E4283. [PubMed: 25246573]
41. Davidson WS, Jonas A, Clayton DF, George JM. Stabilization of alpha-synuclein secondary structure upon binding to synthetic membranes. J. Biol. Chem. 1998; 273:9443–9449. [PubMed: 9545270]
42. Middleton ER, Rhoades E. Effects of curvature and composition on α-synuclein binding to lipid vesicles. Biophys. J. 2010; 99:2279–2288. [PubMed: 20923663]
43. Rhoades E, Ramlall T, Webb W, Eliezer D. Quantification of alpha-synuclein binding to lipid vesicles using fluorescence correlation spectroscopy. Biophys. J. 2006; 90:4692–4700. [PubMed: 16581836]
44. Bussell R Jr, Eliezer D. Effects of Parkinson's disease-linked mutations on the structure of lipid-associated alpha-synuclein. Biochemistry. 2004; 43:4810–4818. [PubMed: 15096050]
45. Bodner C, Dobson C, Bax A. Multiple tight phospholipid-binding modes of alpha-synuclein revealed by solution NMR spectroscopy. J. Mol. Biol. 2009; 390:775–790. [PubMed: 19481095]
46. Bodner C, Maltsev A, Dobson C, Bax A. Differential phospholipid binding of alpha-synuclein variants implicated in Parkinson's disease revealed by solution NMR spectroscopy. Biochemistry. 2010; 49:862–871. [PubMed: 20041693]
47. Dikiy I, Eliezer D. N-terminal Acetylation Stabilizes N-terminal Helicity in Lipid- and Micelle-bound α-Synuclein and Increases Its Affinity for Physiological Membranes. J. Biol. Chem. 2014; 289:3652–3665. [PubMed: 24338013]
48. Pfefferkorn CM, Lee JC. Tryptophan probes at the alpha-synuclein and membrane interface. J Phys Chem B. 2010; 114:4615–4622. [PubMed: 20229987]
49. Middleton ER, Rhoades E. Effects of curvature and composition on alpha-synuclein binding to lipid vesicles. Biophys J. 2010; 99:2279–2288. [PubMed: 20923663]

50. Fares M-B, Ait-Bouziad N, Dikiy I, Mbefo MK, Jovičić A, Kiely A, Holton JL, Lee S-J, Gitler AD, Eliezer D, Lashuel HA. The novel Parkinson's disease linked mutation G51D attenuates in vitro aggregation and membrane binding of α-synuclein, and enhances its secretion and nuclear localization in cells. Hum. Mol. Genet. 2014; 23:4491–4509. [PubMed: 24728187]

51. Gitler AD, Bevis BJ, Shorter J, Strathearn KE, Hamamichi S, Su LJ, Caldwell KA, Caldwell GA, Rochet J-C, McCaffery JM, Barlowe C, Lindquist S. The Parkinson's disease protein α-synuclein disrupts cellular Rab homeostasis. Proc. Natl. Acad. Sci. U.S.A. 2008; 105:145–150. [PubMed: 18162536]

52. Outeiro TF, Lindquist S. Yeast Cells Provide Insight into Alpha-Synuclein Biology and Pathobiology. Science. 2003; 302:1772–1775. [PubMed: 14657500]

53. Kundu K, Mann M, Costa F, Backofen R. MoDPepInt: an interactive web server for prediction of modular domain-peptide interactions. Bioinformatics. 2014; 30:2668–2669. [PubMed: 24872426]

54. Kalia LV, Salter MW. Interactions between Src family protein tyrosine kinases and PSD-95. Neuropharmacol. 2003; 45:720–728.

55. Ysselstein D, Joshi M, Mishra V, Griggs AM, Asiago JM, McCabe GP, Stanciu LA, Post CB, Rochet J-C. Effects of impaired membrane interactions on α-synuclein aggregation and neurotoxicity. Neurobiol. Dis. 2015; 79:150–163. [PubMed: 25931201]

56. Tenreiro S, Reimão-Pinto MM, Antas P, Rino J, Wawrzycka D, Macedo D, Rosado-Ramos R, Amen T, Waiss M, Magalhães F, Gomes A, Santos CuN, Kaganovich D, Outeiro TF. Phosphorylation Modulates Clearance of Alpha-Synuclein Inclusions in a Yeast Model of Parkinson's Disease. PLoS Genet. 2014; 10:e1004302. [PubMed: 24810576]

57. Volles MJ, Lansbury PT Jr. Relationships between the Sequence of α-Synuclein and its Membrane Affinity, Fibrillization Propensity, and Yeast Toxicity. J. Mol. Biol. 2007; 366:1510–1522. [PubMed: 17222866]

58. Snead D, Eliezer D. Alpha-synuclein function and dysfunction on cellular membranes. Exp Neurobiol. 2014; 23:292–313. [PubMed: 25548530]

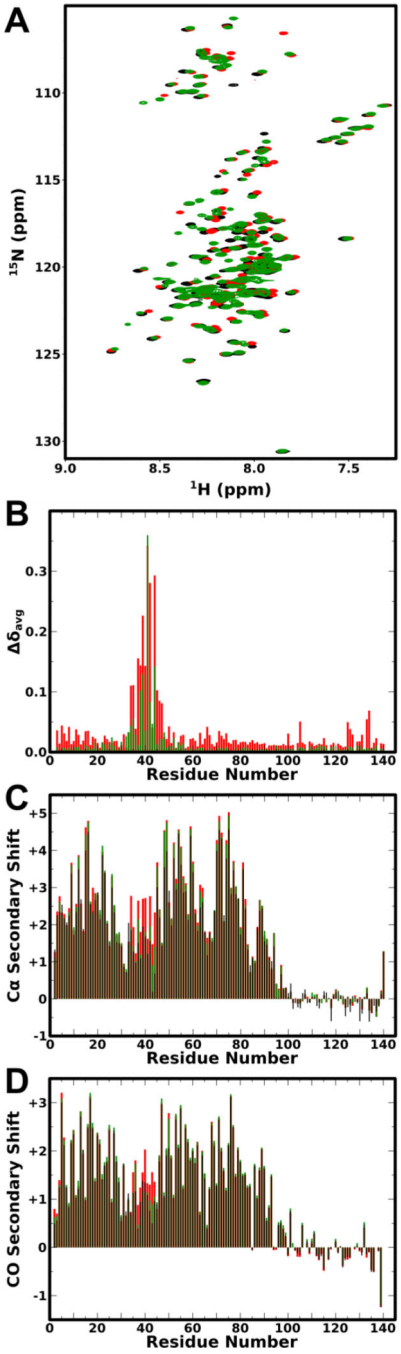

Figure 1. NMR analysis of the effect of Y39 phosphorylation on aSyn binding to SDS micelles

A: ^{1}H,^{15}N-HSQC spectra of WT (black) aSyn, pY39 aSyn Y125F/Y133F (red), and aSyn Y39E (green) in the presence of SDS micelles. **B:** Plot of average amide chemical shift difference between pY39 aSyn Y125F/Y133F and WT aSyn (red) and between aSyn Y39E and WT aSyn (green) in the presence of SDS micelles *versus* residue number. **C:** Plot of Cα secondary shifts for unphosphorylated WT (black), pY39 aSyn Y125F/Y133F (red) and aSyn Y39E (green) in the presence of SDS micelles *versus* residue number. **D:** Plot of CO secondary shifts for unphosphorylated WT (black), pY39 aSyn Y125F/Y133F (red) and

aSyn Y39E (green) in the presence of SDS micelles *versus* residue number. For panels C and D, positive and negative values indicate helical and extended structure, respectively.

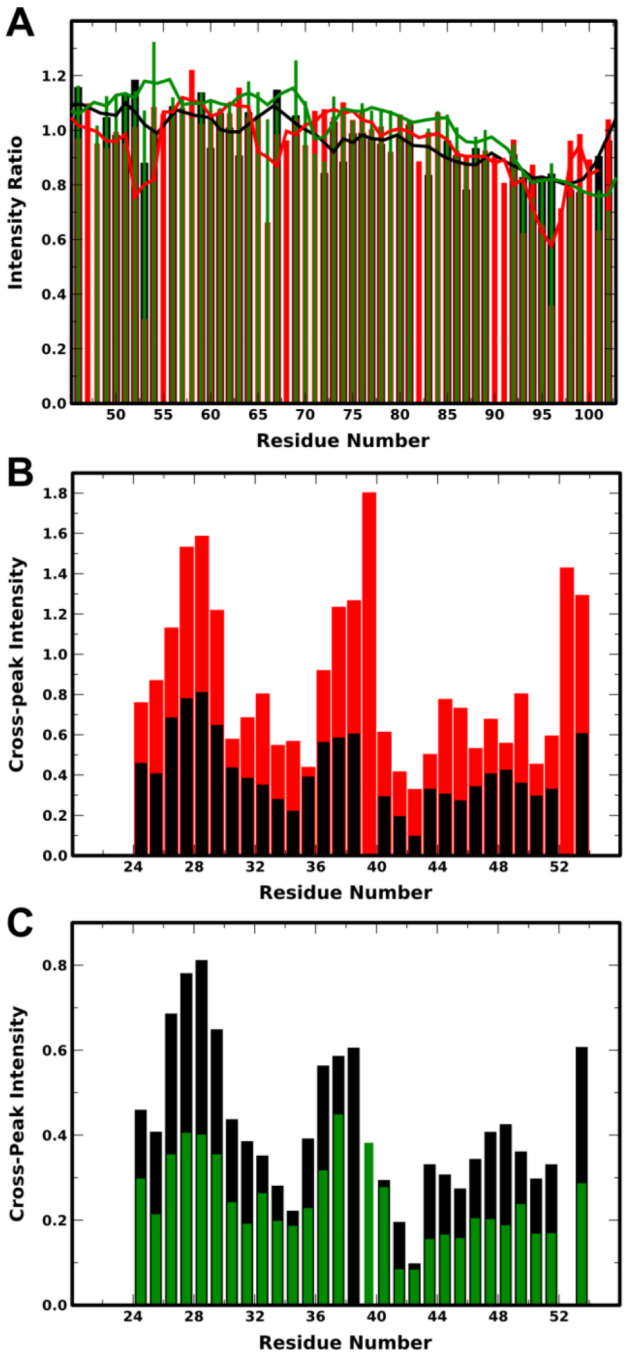

Figure 2. Determination of helical conformation of pY39 aSyn on SDS micelles

A: Plot of ratio of peak intensity of spin-labeled to unlabeled S9C aSyn 1–102 for unphosphorylated (black), pY39 (red) and Y39E (green) protein in the presence of SDS micelles *versus* residue number. Lower peak intensity ratios represent a PRE effect that arises from proximity to the spin-label. For clarity, data are shown only for residues 46–102 because the expected long-range PRE effects occur around position 95. A complete plot is provided in Fig. S7A. Note that some signals could be resolved for one protein variant, but not for others, thus not each residue has data for all three variants. **B:** Plot of average

sequential NH-NH NOE intensities for WT aSyn (black) and pY39 (red) aSyn in the presence of SDS micelles *versus* residue number. **C:** Plot of average sequential NH-NH NOE intensities for WT aSyn (black) and aSyn Y39E (green) in the presence of SDS micelles *versus* residue number. For panels B and C, only residues 24–54, containing the linker region, were analyzed; sequential NH-NH NOEs indicate helical or compact structure; positions with no plotted intensity are due to spectral overlap or difficulty isolating peaks.

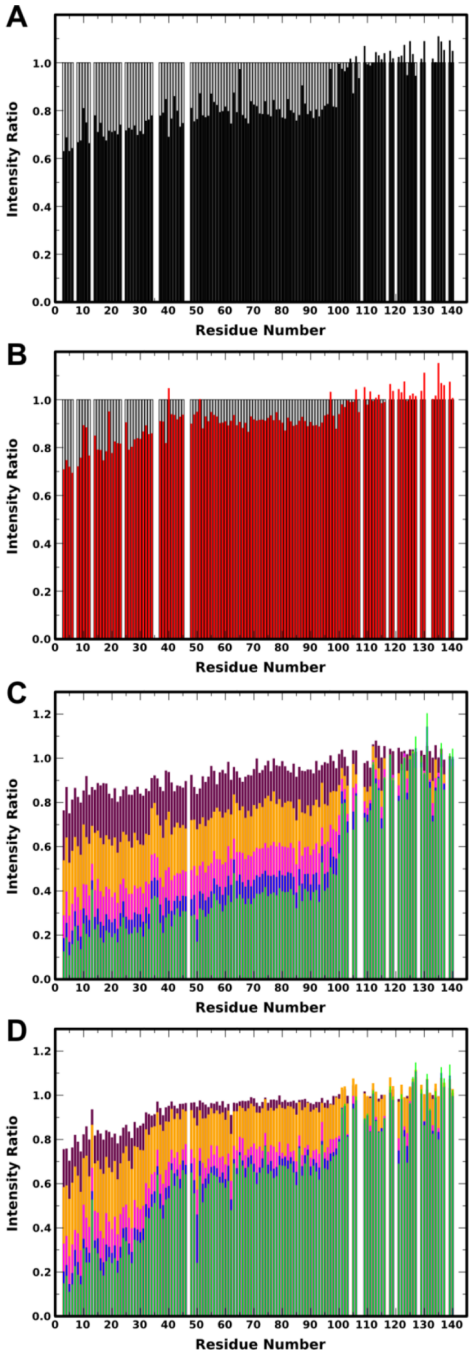

Figure 3. NMR analysis of the effect of Y39 phosphorylation on aSyn binding to lipid vesicles

A,B: Plots of ratio of peak intensities of protein in the presence of 3 mM 15% DOPS/25% DOPE/60% DOPC SUVs to protein without SUVs for unphosphorylated (black, A)and pY39 (red, B) aSyn Y125F/Y133F *versus* residue number. Grey bars indicate which peaks were analyzed and lower intensity ratio reflects a greater population of protein with that region bound. **C,D:** Plot of ratio of peak intensity of protein in the presence of 1.5 (maroon), 3 (orange), 6 (magenta), 9 (blue), and 12 (light green) mM 15% DOPS/25% DOPE/60%

DOPC SUVs to protein without SUVs for WT (C) and Y39E (D) aSyn *versus* residue number. Lower intensity ratio reflects a greater population of protein with that region bound.

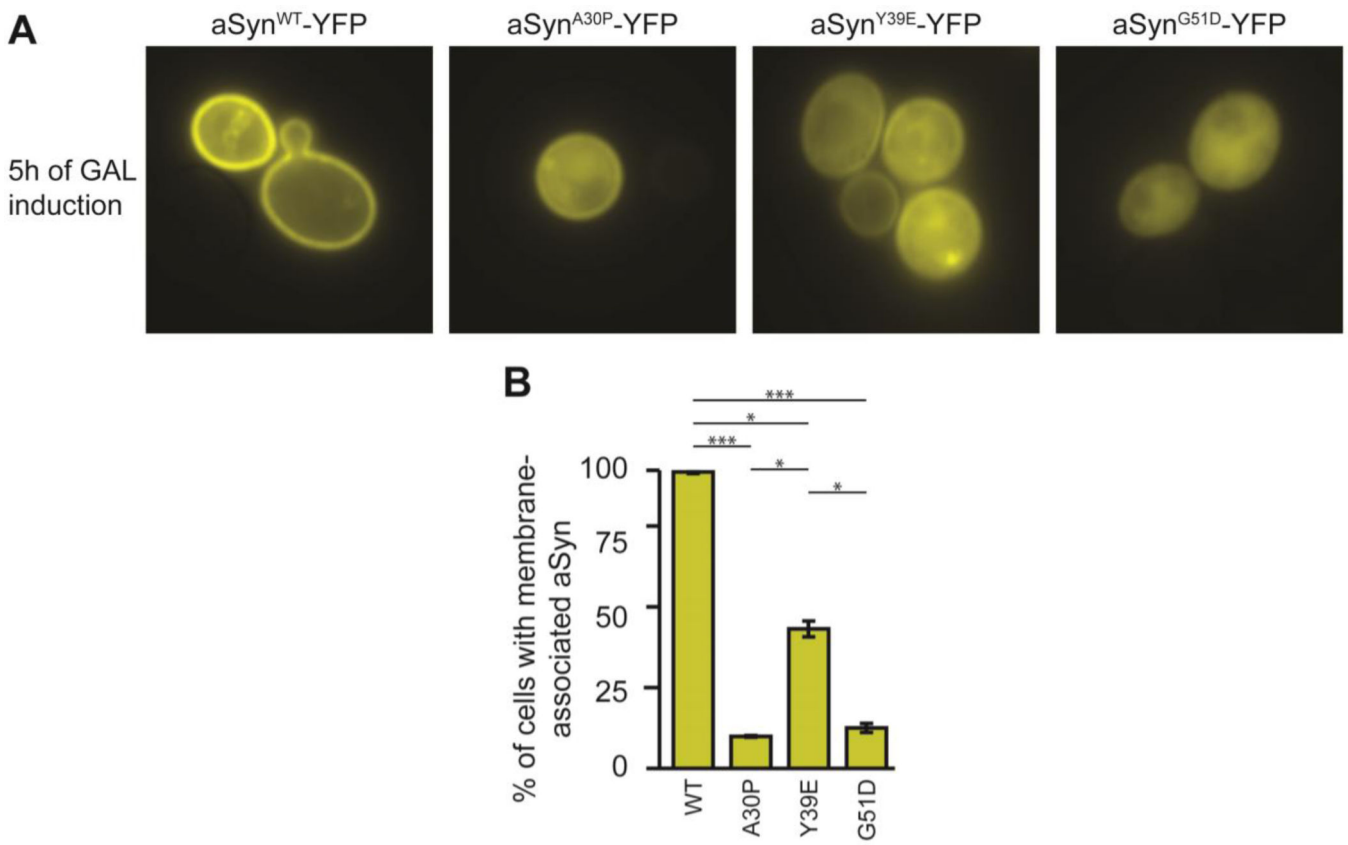

Figure 4. Membrane localization of aSyn y39E in yeast

A: Representative fluorescence microscopy images of yeast overexpressing YFP fusions of aSyn WT, A30P, Y39E, and G51D after 5 hours of induction. **B:** Percentage of cells with membrane-associated aSyn. Values are the mean ± SEM of 3 independent experiments of 5 random fields each; * and *** represent P-values < 0.05 and 0.001, respectively.

Table 1

Populations of different bound states of unphosphorylated and pY39 aSyn Y125F/Y133F in the presence of 3 mM 15% DOPS/25% DOPE/60% DOPC SUVs.

	Populations[a]			K_D Estimate (mM)[b]	
Protein	**All bound states**	**Partly-helical (incl. helix-1)**	**Extended helix**	**All bound states**	**Extended helix**
aSyn Y125F/Y133F	0.377 ± 0.034	0.146 ± 0.093	0.232 ± 0.059	4.9	10
pY39 aSyn Y125F/ Y133F	0.319 ± 0.041	0.176 ± 0.088	0.143 ± 0.047	6.4	18.4

[a] Bound fractions are calculated as described in Methods in SI from Figures 5A and B.

[b] Dissociation constants were estimated from one-point bound populations using equation 3 in the SI.

Table 2

Calculated apparent dissociation constants for different binding states of WT and Y39E aSyn to 15% DOPS/25% DOPE/60% DOPC SUVs.

Protein	All bound states $K_{D,app}$ (mM)[a]	Extended helix $K_{D,app}$ (mM)[a]
WT aSyn	3.8 ± 0.5	9.9 ± 1.0
aSyn Y39E	3.4 ± 0.4	26.0 ± 1.1

[a]Apparent dissociation constants are calculated from fitting the bound fractions, calculated as described in Methods in SI from Figures 6C and D, to equation 3.